Supporting Information

Asymmetric end-capping strategy enables new non-fullerene acceptor for organic solar cells with efficiency over 10%

Tainan Duan,† Licheng Hou,† Jiehao Fu, Zhipeng Kan, Qianguang Yang, Qianqian Chen, Cheng Zhong, Zeyun Xiao, Donghong Yu* and Shirong Lu**

Content:

1. General Experimental Details

All reactions were performed under nitrogen atmosphere and solvents were purified and dried from appropriate drying agents using standard techniques prior to use. Reagents available from commercial sources were used without further purification unless otherwise stated. Flash chromatography was performed by using Silicycle Silica Flash P60 (particle size 40-63 μm, 60 Å, 230-400 mesh) silica gel. Silica gel on TLC-PET foils from Fluka was used for TLC. Recycling SEC in THF or ethanol-stabilized chloroform was carried out through a set of two JAIGEL-4H-40 preparative SEC columns mounted on an LC-9130NEXT (JAI) system equipped with coupled UV-254NEXT and RI-700NEXT detectors. 7-bromobenzo[c][1,2,5]thiadiazole-4-carbaldehyde (compound **1)** and di-brominated IDT monomer **3** were purchased from Derthon Optoelectronic Materials Science Technology Co., Ltd. All new compounds were characterized by NMR spectroscopy on a Bruker Avance III Ultrashield Plus instrument (600 MHz), the spectra were referenced on the internal standard TMS. FT-IR spectra were recorded on a PerkinElmer Spectrum Two FT-IR spectrometer. High-resolution mass spectrometry (HR-MS) data of IDTBF was recorded using a Bruker SolariX 70 FT-MS.

2. Synthetic Protocols and Characterizations
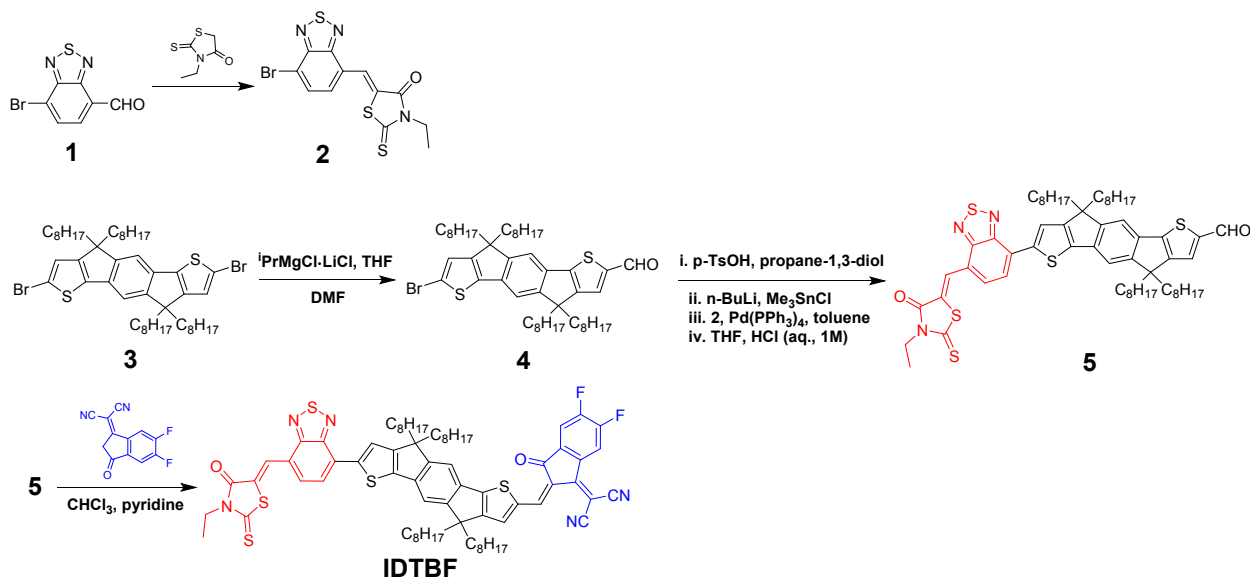
Scheme S1. Synthesis of SM acceptor **IDTBF**.

Note: Compounds **2**[1] was prepared according to previously report procedures.
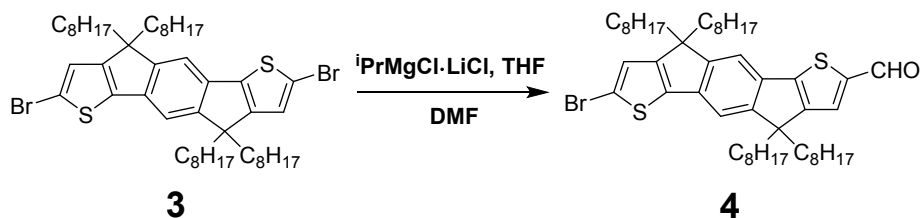
7-bromo-4,4,9,9-tetraoctyl-4,9-dihydro-s-indaceno[1,2-*b*:5,6-*b'*]dithiophene-2-carbaldehyde (4): In a pre-dried Schlenk tube, a solution of di-brominated IDT monomer **3** (2.0 g, 2.3 mmol) in anhydrous THF (50 mL) was cooled to 0 °C. A solution of Turbo Grignard reagent ^{i}PrMgCl.LiCl (1.3 M in THF, 2.0 mL, 2.6 mmol) was added dropwise, and the ice bath was removed. The mixture was stirred for 30 min at room temperature, and was then heated to reflux for 30 min. The heating bath was removed and anhydrous DMF (0.46 mL, 6.0 mmol) was added to the reaction mixture in one portion. After being stirred overnight, the reaction was quenched with HCl (1 M in water, 20 mL) and the aqueous phase was extracted with ethyl acetate (2 × 50 mL). The organic phase was separated, dried over Na_2SO_4 and then concentrated under reduced pressure. The crude product was purified by column chromatography over SiO_2 using PE/DCM

(v/v = 1/1) as the eluent. The solvent was removed by rotary evaporation, affording aldehyde **4** as an orange solid (1.23 g, yield: 65%). ^{1}H NMR (600 MHz, CDCl$_3$, δ ppm): 9.88 (s, 1H), 7.61 (s, 1H), 7.38 (s, 1H), 7.23 (s, 1H), 7.00 (s, 1H), 2.01-1.93 (m, 4H), 1.88-1.86 (m, 4H), 1.21-1.10 (m, 40H), 0.83-0.77 (m, 12H). ^{13}C NMR (150 MHz, CDCl$_3$, δ ppm): 182.79, 155.29, 155.17, 155.02, 152.61, 152.35, 144.67, 141.48, 137.99, 134.11, 130.40, 124.88, 114.88, 113.94, 113.13, 54.88, 54.12, 38.97, 38.91, 31.77, 29.89, 29.24, 29.17, 29.15, 24.25, 24.12, 22.58, 22.58, 14.03. HR-MS (+APCI, m/z): calcd. for C$_{49}$H$_{73}$BrNaOS$_2$$^+$ [M+Na]$^+$: 843.41784, found 843.41793.

(*E*)-7-(7-((3-ethyl-4-oxo-2-thioxothiazolidin-5-ylidene)methyl)benzo[c][1,2,5]thiadiazol-4-yl)-4,4,9,9-tetraoctyl-4,9-dihydro-s-indaceno[1,2-*b*:5,6-*b*']dithiophene-2-carbaldehyde (5):

Step 1: To a solution of aldehyde **4** (1.0 g, 1.22 mmol mmol) and 1,3-propanediol (0.93 g, 12.2 mmol) in toluene (30 mL) was added *p*-toluenesulfonic acid (200 mg). This mixture was refluxed for 8 h in a Dean-Stark apparatus to remove the theoretical amount of water. Then the solution was washed with 1 M aqueous NaHCO$_3$ and then with water, dried over MgSO$_4$, and concentrated in a vacuum to give the 1,3-propanediol acetal (1.02 g, yield: 95%) as a brown oil, which was sufficiently pure to be used in the next step.

Step 2: In a pre-dried round flask, a solution of the 1,3-propanediol acetal (1.02 g, 1.16 mmol) in anhydrous THF (25 mL) was cooled to -78 °C. A solution of *n*-BuLi (1.6 M in hexane, 0.87 mL, 1.39 mmol) was added dropwise, and the mixture was stirred for 1 h at -78 °C. Next, trimethyltin chloride in THF (1.0 M, 1.66 mL, 1.66 mmol) was added to the mixture in one portion. The cooling bath was then removed, the mixture was allowed to warm to room temperature, and was stirred overnight. The reaction was quenched with saturated KF solution (100 mL) and the aqueous phase was extracted with dichloromethane (2 × 50 mL). The organic phase was collected, dried over Na$_2$SO$_4$, concentrated under reduced pressure, and tin-acetal reagent (1.03 g, yield: 92%) was obtained as a brown oil and subjected to the next step without further purification.

Step 3 and step 4: In a pre-dried Schlenk flask, tin-acetal reagent (1.03 g, 1.06 mmol), brominated BR (compound **2**) (452 mg, 1.17 mmol) and Pd(PPh$_3$)$_4$ (98 mg, 0.08 mmol) were dissolved in pre-degassed toluene (30 mL). The reaction mixture was heated to 110 °C and stirred for 48 h. Next, the mixture was concentrated under reduced pressure, and then mixed with 1 M HCl (60 mL) to stir for 6 h. Then, the organic phase was extracted with dichloromethane (2 × 50 mL), washed with brine, dried over anhydrous Na$_2$SO$_4$ and the solvent was evaporated. Finally, the BR end-capped aldehyde **5** was roughly purified once by column chromatography over SiO$_2$ using PE/DCM (v/v = 2/3) as the eluent, giving a brown solid (497 mg, yield: 46%). ^{1}H NMR (600 MHz, CD$_2$Cl$_2$, δ ppm): 9.80 (s, 1H), 8.40 (s, 1H), 8.16 (s, 1H), 7.98 (d, J = 7.8 Hz, 1H), 7.68 (d, J = 7.8 Hz, 1H), 7.58 (s, 1H), 7.44 (s, 1H), 7.42 (s, 1H), 4.17 (q, J = 7.2 Hz, 2H), 2.07-1.97 (m, 4H), 1.94-1.84 (m, 4H), 1.24 (t, J = 7.2 Hz, 3H), 1.12-1.03 (m, 40H), 0.74-0.68 (m, 12H).

2-((Z)-2-((7-(7-((E)-(3-ethyl-4-oxo-2-thioxothiazolidin-5-ylidene)methyl)benzo[c][1,2,5]thiadiazol-4-yl)-4,4,9,9-tetraoctyl-4,9-dihydro-s-indaceno[1,2-b:5,6-b']dithiophen-2-yl)methylene)-5,6-difluoro-3-oxo-2,3-dihydro-1H-inden-1-ylidene)malononitrile (IDTBF): To a solution of compound **5** (300 mg, 0.28 mmol), 2-(5,6-difluoro-3-oxo-2,3-dihydro-1H-inden-1-ylidene)malononitrile (97 mg, 0.42 mmol) in anhydrous CHCl$_3$ (30 mL), several drops of anhydrous pyridine was added. The mixture was heated at 60 °C for *ca.* 4 hours. After cooling to room temperature, the mixture was concentrated to *ca.* 5 mL and poured into methanol (50 mL) and then filtered. The residue was collected and purified by column chromatography over SiO$_2$ using PE/CHCl$_3$ (v/v = 1/2) as the eluent to afford final product **IDTBF** as a blue solid (317 mg, yield: 88%).^{1}H NMR (600 MHz, CD$_2$Cl$_2$, δ ppm): 8.88 (s, 1H), 8.46 (m, 1H), 8.40 (s, 1H), 8.17 (s, 1H), 8.00 (d, J = 7.8 Hz, 1H), 7.70-7.68 (m, 2H), 7.63-7.60 (m, 2H), 7.44 (s, 1H), 4.16 (q, J = 7.2 Hz, 2H), 2.09-2.00 (m, 4H), 1.97-1.88 (m, 4H), 1.24 (t, J = 7.2 Hz, 3H), 1.12-1.04 (m, 40H), 0.73-0.68 (m, 12H). ^{13}C NMR (150 MHz, CHCl$_3$, δ

ppm): 192.91, 186.02, 167.53, 163.62, 158.77, 157.01, 154.82, 154.55, 151.75, 145.03, 142.99, 140.11, 138.70, 134.87, 131.15, 130.05, 127.00, 125.12, 124.96, 124.40, 123.84, 119.93, 116.12, 114.65, 114.11, 68.36, 54.50, 54.29, 39.97, 39.17, 39.02, 31.79, 29.95, 29.91, 29.29, 29.21, 24.40, 24.33, 22.60, 14.08, 14.06, 12.34. ^{19}F (^{1}H decoupled) NMR (565 MHz, CD$_2$Cl$_2$, δ ppm): -125.01 (d, J = 19.21 Hz, 1F), -126.00 (d, J = 19.21 MHz, 1F). HR-MS (+APCI, m/z): calcd. for C$_{73}$H$_{83}$F$_2$N$_5$O$_2$S$_5$$^+$ [M+H]$^+$: 1260.51911, found 1260.51914.

3. Thermogravimetric Analysis (TGA)

Thermogravimetric Analysis (TGA) was performed with a Mettler-Toledo TGA/DSC 3+ analyzer under a nitrogen atmosphere, using aluminum crucibles.
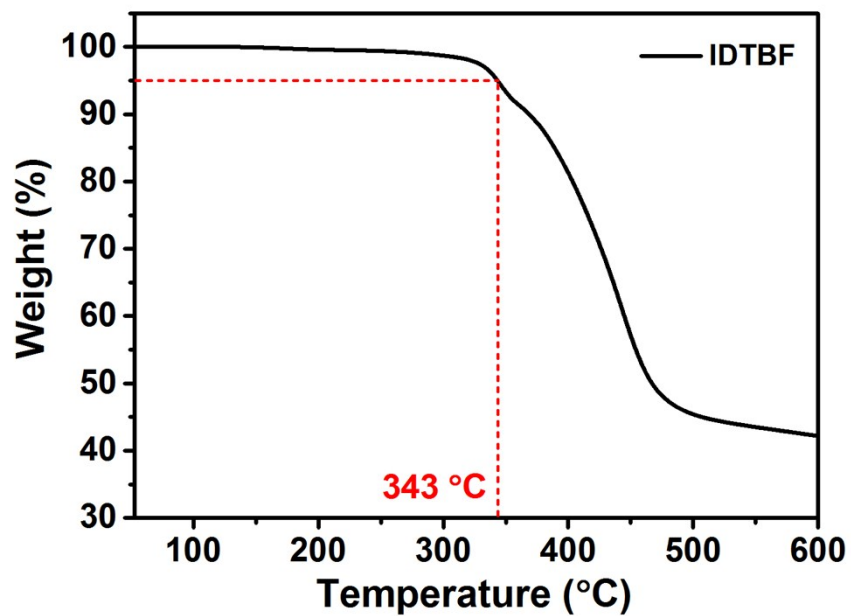
Figure S1. Thermogravimetric analysis (TGA) of **IDTBF**. The molecular acceptor shows good thermal-stability under nitrogen atmosphere; *ca.* 5% weight loss observed at 343 °C.

4. Differential Scanning Calorimetry (DSC) Measurements

Differential Scanning Calorimetry (DSC) measurements were performed on a Mettler-Toledo TGA/DSC 3+ analyzer under a nitrogen atmosphere, using aluminum crucibles.
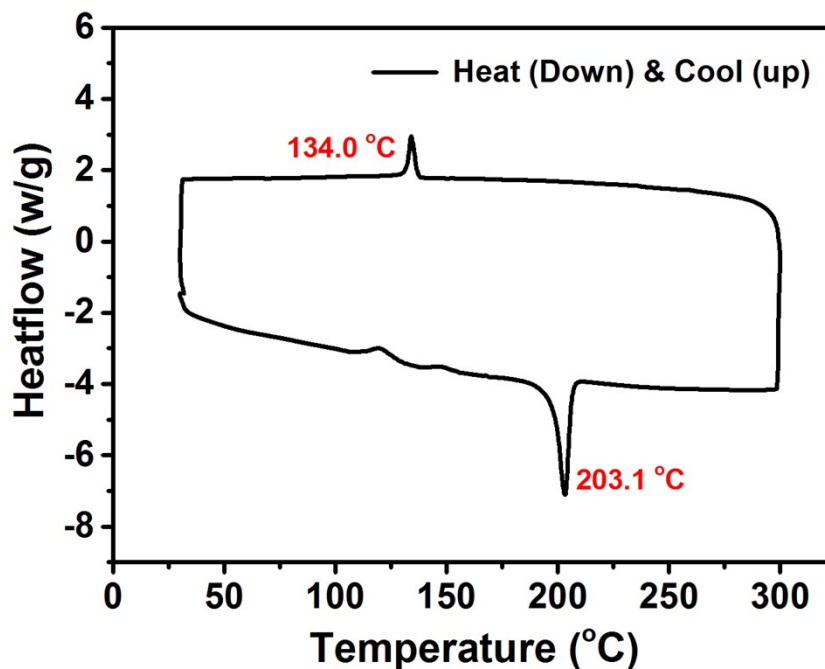
Figure S2. Differential Scanning Calorimetry (DSC) trace of **IDTBF**. Analysis carried out with a scan rate of 10 °C/min between 30 °C and 300 °C. The SM acceptor shows an apparent phase transition around 203 °C and 134 °C, respectively, suggesting a melt transition in light of the presence of a first order solidification peak on the cooling scan.

5. Density Functional Theory (DFT) Calculations

The density functional theory (DFT) calculations were performed at the ω-tuned wb97x/def2TZVP level based on PBE0-D3BJ/def2-SVP optimized geometry with the Gaussian 09 (Revision E.01) code. The side chains were modeled as methyl groups; while side chains play an important role in the organization of small molecules and polymers in the solid state, these have only marginal influence on the electronic and optical properties of the single isolated small-molecule/polymer chain in the gas phase.
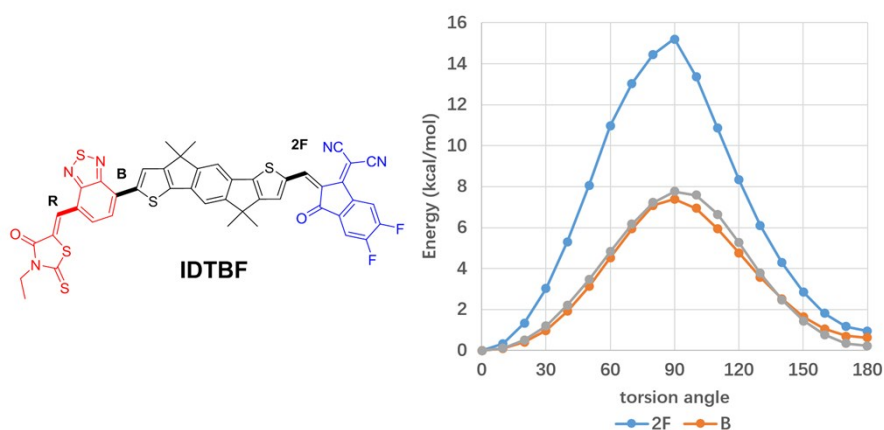
Figure S3. The torsion potential of three ratable bonds in IDTBF. The torsion potential shows that the rotation barrier and the rotation conformer energy of "IDT --- IM2F" is higher than "IDT --- BR". This will lead to a more planar geometry with less structural disorder.
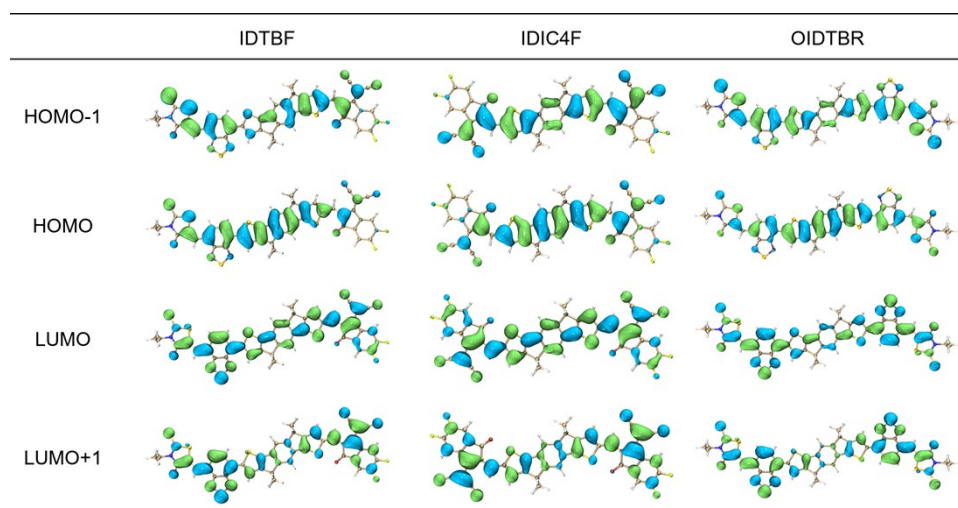
Figure S4. Frontier orbitals distribution of three SM acceptors.

Table S1. Frontier orbital energy levels of three SM acceptors.

SM acceptor	HOMO-1 (eV)	HOMO (eV)	LUMO (eV)	LUMO+1 (eV)
IDIC-4F	-7.07	-6.29	-3.79	-3.38
IDTBF	-6.58	-5.90	-3.57	-3.27
o-IDTBR	-6.20	-5.60	-3.39	-3.18

Table S2. The transition properties (energy, oscillator strength, and orbital composition) of first three excited states of SM acceptors.

SM acceptor	Sn	Transition Energy (eV)	Wave length (nm)	Osc. strength	Orbital composition
IDIC-4F	1	2.14	580.49	2.462	H-L:0.981
	2	2.55	486.12	0	H-L1:0.922
	3	2.81	441.52	0.1609	H-L2:0.908
IDTBF	1	1.96	631.33	2.3927	H-L:0.972
	2	2.32	535.25	0.0125	H-L1:0.95
	3	2.59	479.19	0.0001	H2-L:0.624
o-IDTBR	1	1.84	674.8	2.3806	H-L:0.973
	2	2.13	582.86	0	H-L1:0.981
	3	2.50	495.94	0	H1-L:0.943

6. UV-Vis Spectroscopy

UV-Vis spectra of solution and thin films were recorded on a PerkinElmer LAMBDA 365 UV-Vis spectrophotometer.
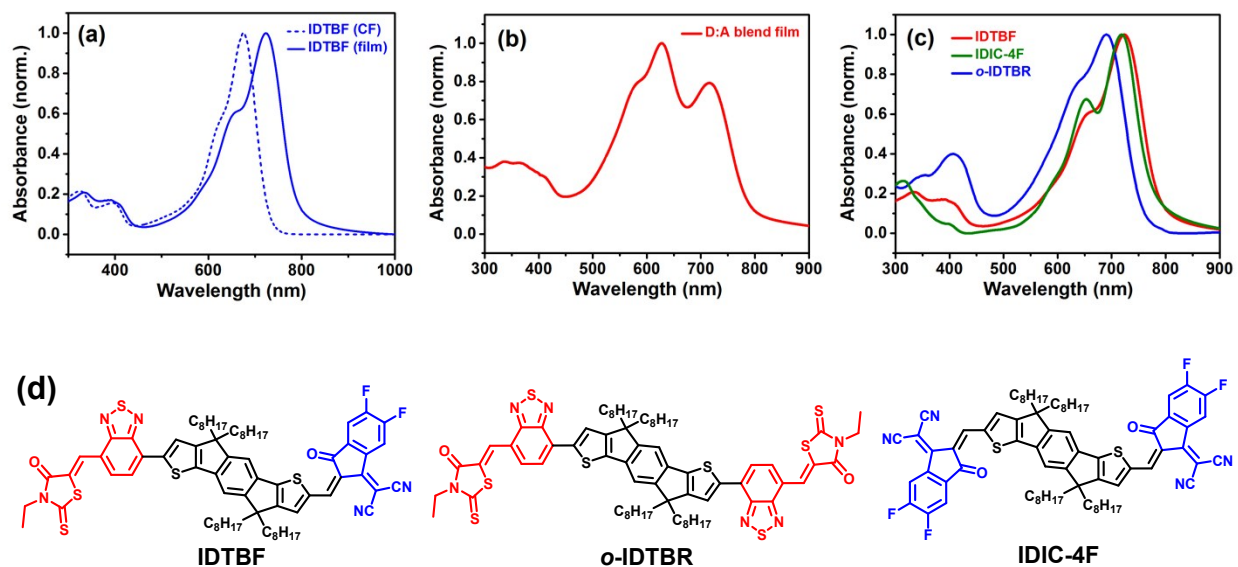
Figure S5. **(a)** Normalized UV-vis spectra of chloroform solution and thin film of **IDTBF**. **(b)** Normalized UV-Vis absorption spectra of optimized bulk-heterojunction **PM6**:**IDTBF** blend film. **(c)** Normalized UV-vis spectra of as-cast thin film of *o*-**IDTBR**, **IDIC-4F** and **IDTBF**. **(d)** Molecule structures of SM acceptors *o*-**IDTBR**, **IDIC-4F** and **IDTBF**.

7. Photoluminescence Spectroscopy (PL)

Photoluminescence spectra of **IDTBF** were measured on a PerkinElmer LS-45 fluorescence spectrometer.
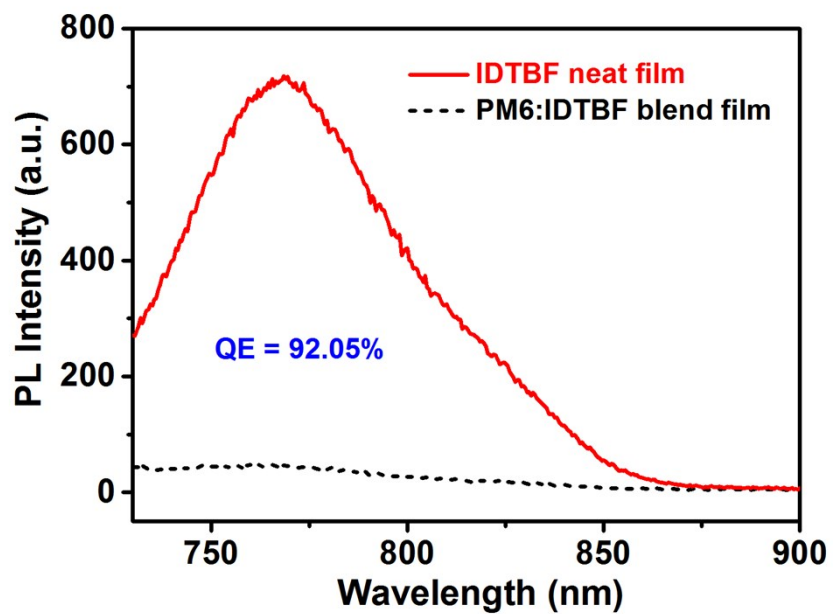
Figure S6. PL spectra of the neat **IDTBF** film and **PM6**:**IDTBF** blend film.

8. Device Fabrication

The BHJ solar cells were prepared on the glass substrates with tin-doped indium oxide (ITO, 15Ω/sq) on part of the surface and the effective area of each device is 0.11cm^2. The entire cleaning process of the substrates can be divided into four sections. At first, the substrates were prewashed with detergent in an Ultrasonic cleaning machine for 15 min to remove the stains. Then deionized water was used to wash the detergent left on the substrates. Followed by this, the substrates were cleaned by acetone for 15 min in the ultrasonic bath. At last, isopropanol was applied to remove organic residues before immersing in an ultrasonic bath for 15 min. Next, the samples were dried with pressurized nitrogen before being exposed to a UV-ozone plasma for 20 min. A thin layer (~35nm) of PEDOT:PSS was spin cast onto the UV-treated samples, dried on the hot plate at 160 °C for 15 minutes, and then transferred into a dry nitrogen glovebox (< 3 ppm O$_2$).

All solutions were prepared in a glovebox. Polymer donors P3HT, PCE10 and PM6 are purchased from Derthon Optoelectronic Materials Science Technology Co., Ltd. Optimized devices were obtained by dissolving the polymer donor and IDTBF in chlorobenzene. The as-prepared solutions were stirred 3 hours at 40 °C before being cast. The effects of blend ratios and different post-conditions such as thermal annealing (TA) and solvent vapor annealing (SVA) on the device performance were also examined.

Next, the samples were dealt with optimized conditions. The active layers were spin-cast from the solutions of PM6:IDTBF at 40 °C at a single substrate. Then each substrates was exposed to chloroform steam (which was put into a glass Petri dish of 6 cm diameter) for 20 sec. Next, the Phen-NaDPO which was used as the electron transporting layer was spin-coated on the active layer on a speed of 2000 rpm from isopropyl alcohol solution. The samples were then dried at room temperature for 20min. At the final period, the substrates were pumped down in high vacuum at a pressure of 3×10^{-4} Pa, and Ag layer (100 nm) was thermally evaporated onto the active layer. Shadow masks were used to define the OSC active area (0.11 cm^2) of the devices. Following electrode deposition process, samples underwent $J-V$ testing.

The current density–voltage (J–V) characteristics of unencapsulated photovoltaic devices were measured under N$_2$ using a Keithley 2400 source meter. A 300 W xenon arc solar simulator with an AM 1.5 global filter operated at 100 mW cm^{-2} was used to simulate the AM 1.5G solar

irradiation. The illumination intensity was corrected by using a silicon photodiode with a protective KG5 filter calibrated by the National Renewable Energy Laboratory (NREL). The external quantum efficiency (EQE) was performed using certified IPCE equipment (Zolix Instruments, Inc, Solar Cell Scan 100).

9. Additional PV Device Performance Data
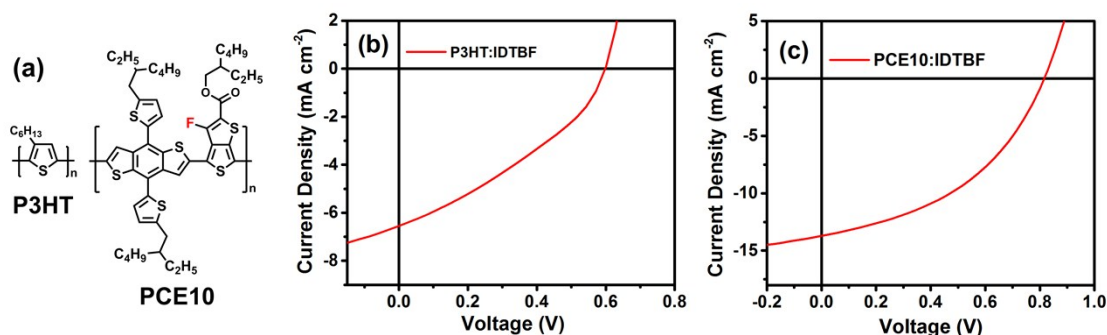
Figure S7. **(a)** Molecule structures of polymer donors **P3HT** and **PCE10**. **(b)** *J-V* curves of solar cells made with of **P3HT**:**IDTBF** blend film. **(c)** *J-V* curves of solar cells made with of **PCE10**:**IDTBF** blend film.

Table S3. Photovoltaic properties of the optimized **P3HT**:**IDTBF** and **PCE10**:**IDTBF** devices.

Blend	V_{OC} (V)	J_{SC} (mA/cm^2)	FF (%)	PCE$_{ave.}$ (%)	PCE$_{max.}$ (%)
P3HT:IDTBF	0.57±0.00	6.40±0.28	35.18±1.75	1.29±0.07	1.35
PCE10:IDTBF	081±0.02	13.67±0.05	45.34±1.47	5.05±0.24	5.29
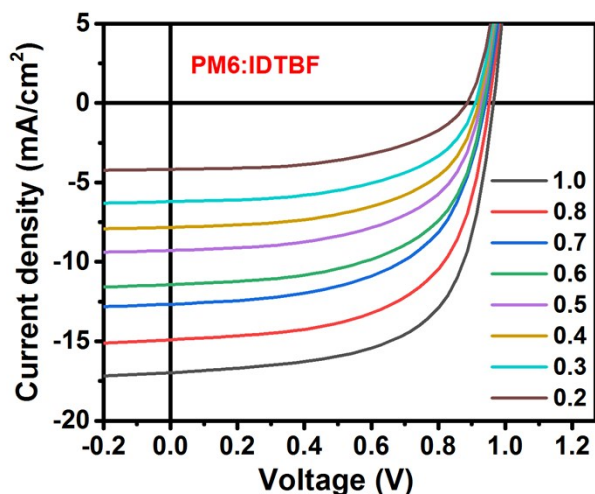
Figure S8. (a) *J-V* curves of BHJ solar cells made with **PM6**:**IDTBF** under different light intensities.

Table S4. Donor-Acceptor ratio dependence for PM6:IDTBF devices. Performance includes standard deviation across at least 10 devices.

D:A ratio (w/w, as cast)	V_{OC}(V)	J_{SC} (mA/cm^2)	FF (%)	PCE$_{ave.}$ (%)	PCE$_{max.}$ (%)
1.5:1	0.93±0.02	15.81±0.24	49.04±1.31	7.22±0.44	7.38
1:1	**0.94±0.00**	**17.29±0.17**	**54.76±2.08**	**8.93±0.60**	**9.27**
1:1.5	0.95±0.02	15.85±0.65	58.82±3.49	8.82±0.34	9.16

Table S5. Spin-coat temperature dependence for PM6:IDTBF devices used chlorobenzene (CB) as the solvent (D:A ratio is kept as 1:1). Performance includes standard deviation across at least 10 devices.

Temperature (as cast)	V_{OC}(V)	J_{SC} (mA/cm^2)	FF (%)	PCE$_{ave.}$ (%)	PCE$_{max.}$ (%)
r.t.	0.87±0.02	16.72±0.15	47.61±0.13	6.94±0.07	7.01
40 °C	**0.94±0.00**	**17.29±0.17**	**54.76±2.08**	**8.93±0.60**	**9.27**
60 °C	0.92±0.03	16.80±0.95	51.14±3.40	7.85±0.41	8.26

Table S6. Thermal annealing (TA) condition dependence for PM6:IDTBF devices used chlorobenzene (CB) as the solvent (D:A ratio is kept as 1:1). Performance includes standard deviation across at least 10 devices.

Temperature	V_{OC}(V)	J_{SC} (mA/cm^2)	FF (%)	PCE$_{ave.}$ (%)	PCE$_{max.}$ (%)
As cast	**0.94±0.00**	**17.29±0.17**	**54.76±2.08**	**8.93±0.60**	**9.27**
TA, 80 °C, 10 min	0.91±0.01	17.70±0.26	52.51±2.33	8.43±0.33	8.67
TA, 100 °C, 10 min	0.86±0.02	18.07±1.34	48.20±4.20	7.49±0.72	8.39
TA, 120 °C, 10 min	0.88±0.01	17.94±0.12	51.32±3.11	7.86±0.42	8.28

Table S7. Solvent vapor annealing (SVA) condition dependence for PM6:IDTBF devices used chlorobenzene (CB) as the solvent (D:A ratio is kept as 1:1). Performance includes standard deviation across at least 10 devices (DMDS = Dimethyl Disulfide).

Solvent	V_{OC} (V)	J_{SC} (mA/cm²)	FF (%)	PCE$_{ave.}$ (%)	PCE$_{max.}$ (%)
None	0.94±0.00	17.29±0.17	54.76±2.08	8.93±0.60	9.27
Chloroform	**0.94±0.00**	**17.13±0.56**	**63.26±3.38**	**10.21±0.23**	**10.43**
THF	0.91±0.02	16.95±0.62	51.75±4.63	8.00±0.78	8.66
CS$_2$	0.93±0.02	15.91±0.21	52.33±2.69	7.71±0.42	8.07
DMDS	0.91±0.01	16.63±0.72	50.43±1.90	7.60±0.22	7.75

Table S8. SVA duration (with chloroform) dependence for PM6:IDTBF devices used chlorobenzene (CB) as the solvent (D:A ratio is kept as 1:1). Performance includes standard deviation across at least 10 devices.

Time (s)	V_{OC} (V)	J_{SC} (mA/cm²)	FF (%)	PCE$_{ave.}$ (%)	PCE$_{max.}$ (%)
10	0.95±0.01	15.98±0.25	58.48±1.32	8.89±0.55	9.08
20	**0.94±0.00**	**17.13±0.56**	**63.26±3.38**	**10.21±0.23**	**10.43**
30	0.93±0.01	14.60±0.08	64.81±0.27	8.83±0.03	8.86
60	0.94±0.01	12.33±0.08	64.19±0.42	7.40±0.14	7.53

Table S9. Additive dependence for PM6:IDTBF devices used chlorobenzene (CB) as the solvent (D:A ratio is kept as 1:1). Performance includes standard deviation across at least 10 devices.

Additive	V_{OC} (V)	J_{SC} (mA/cm²)	FF (%)	PCE$_{ave.}$ (%)	PCE$_{max.}$ (%)
1% DIO	0.70±0.01	9.01±0.05	32.48±0.74	2.05±0.07	2.07
None	**0.94±0.00**	**17.13±0.56**	**63.26±3.38**	**10.21±0.23**	**10.43**
1% CN	0.91±0.00	12.81±0.64	60.73±1.06	7.11±0.36	7.47

10. Carrier Recombination Analysis
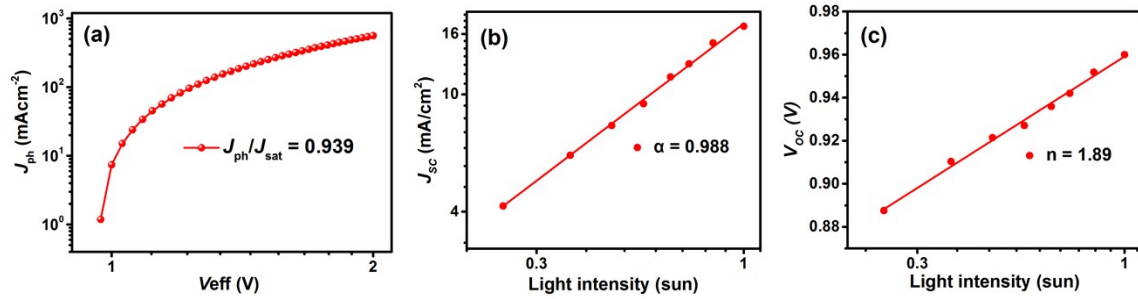
Figure S9. **(a)** J_{ph} *vs.* V_{eff} (effective voltage). J_{ph} is defined as the photocurrent density difference between illuminated and dark conditions ($V_{eff} = V_0 - V$, where V_0 is the voltage when photocurrent reaches zero and V is the applied voltage). When J_{ph} reaches saturation (J_{sat}), the charge dissociation probability can be calculated from J_{ph}/J_{sat}. **(b)** J_{SC} *vs.* light intensity for optimized device. The solid lines correspond to the fits derived from the expression: $J_{SC} \propto I^{\alpha}$. With $\alpha = 0.988$ for **PM6**:**IDTBF**. Note: bimolecular recombination is not the main limiting factor suppressing efficiency for the optimized blends. **(c)** V_{OC} *vs.* light intensity for optimized devices. The solid lines corresponding to the fits derived from the expression: $V_{OC} \propto n\dfrac{kT}{q}ln(I)$. With n = 1.89 for **PM6**:**IDTBF**.

11. Carrier Mobility Measurements

The carrier mobility (hole and electron mobility) of photoactive active layer was obtained by fitting the dark current of hole/electron-only diodes to the space-charge-limited current (SCLC) model. Hole-only diode configuration: Glass/ITO/PEDOT:PSS/PM6:IDTBF/MoO$_3$/Ag; here, V$_{bi}$ = 0 V (flat band pattern formed by PEDOT:PSS-MoO$_3$). Electron-only diode configuration: Glass/ITO/ZnO/DPO/PM6:IDTBF/DPO/Ag; here, V$_{bi}$ = 0.5V was used following the protocol reported.[2] The active layer thickness was determined by a Tencor surface profilometer. The electric-field dependent SCLC mobility was estimated using the following equation:

$$J(V) = \frac{9}{8}\varepsilon_0\varepsilon_r\mu_0 exp\left(0.89\beta\sqrt{\frac{V - V_{bi}}{L}}\right)\frac{(V - V_{bi})^2}{L^3}$$
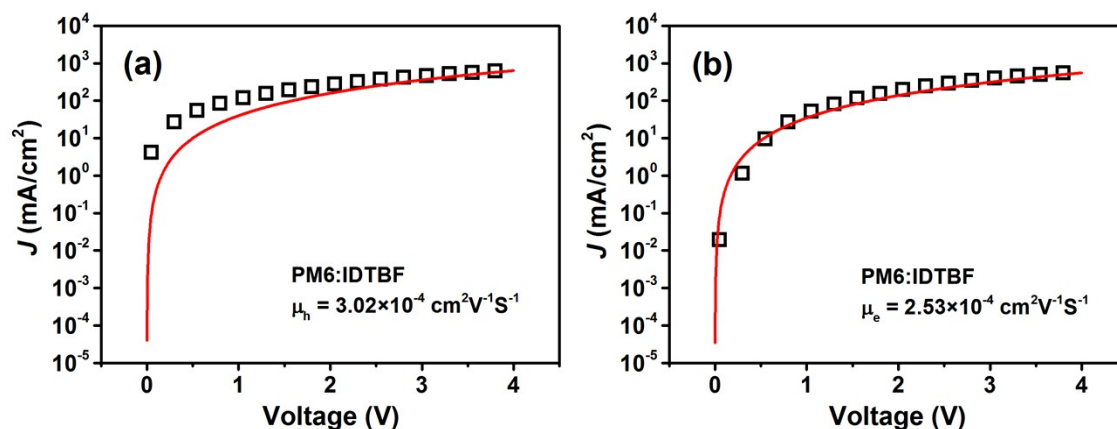
Figure S10. **(a)** hole mobility and **(b)** electron mobility fitting examples of PM6:IDTBF.

Table S10. Average mobility values of devices of PM6:IDTBF.

Blend	μ_h (cm^{2}V^{-1}s^{-1})	μ_e (cm^{2}V^{-1}s^{-1})
PM6:IDTBF	3.02×10^{-4}	2.53×10^{-4}

12. Atomic Force Microscopy (AFM) Imaging
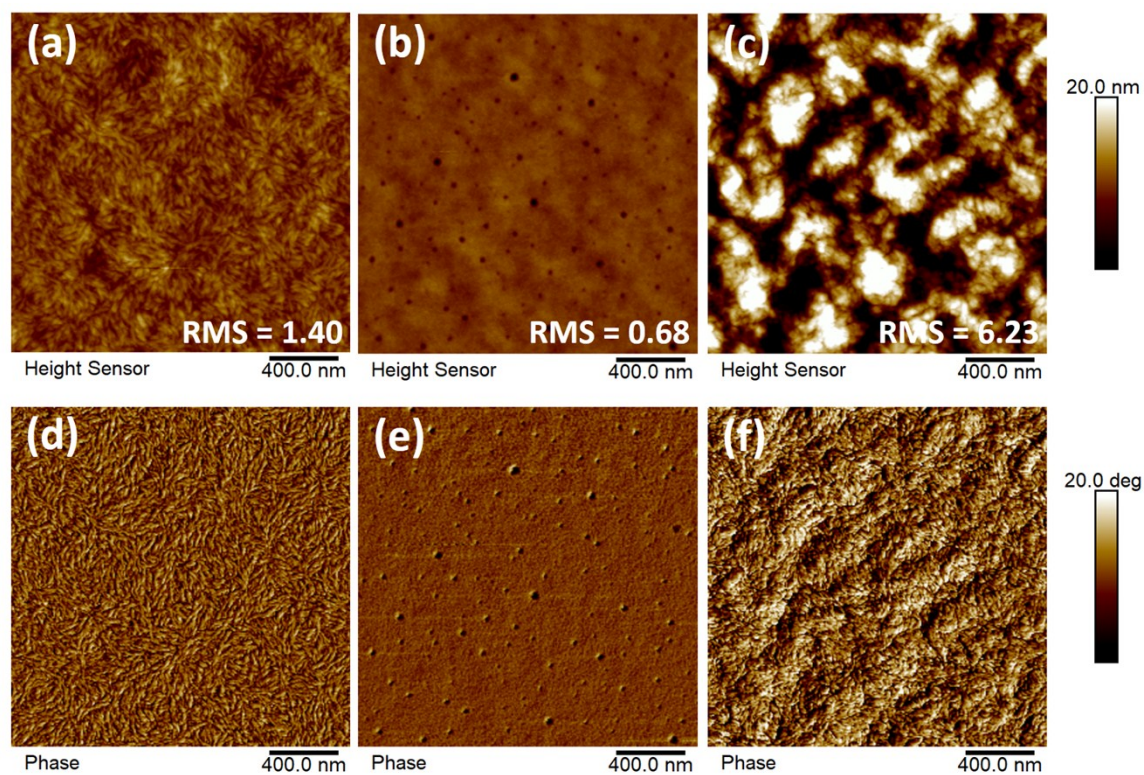
Figure S11. Topography and phase images (tapping mode) of **(a, d)** pristine film of PM6, **(b, e)** pristine film of IDTBF and **(c, f)** optimized blend film of **PM6**:**IDTBF**.

13. Transmission Electron Microscopy (TEM) Imaging
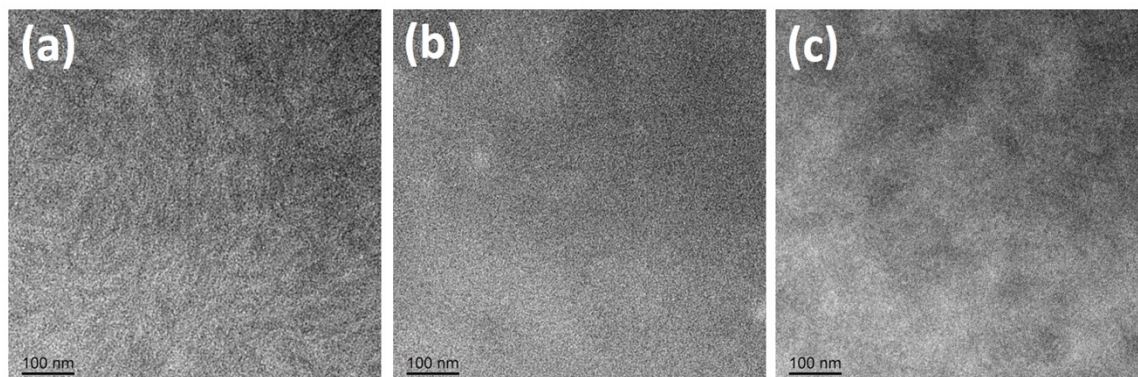
Figure S12. Bright-field TEM images of **(a)** pristine film of PM6, **(b)** pristine film of IDTBF and **(c)** optimized blend film of **PM6**:**IDTBF**. Scale bar is 100nm.

14. Solution NMR and HR-MS Spectra
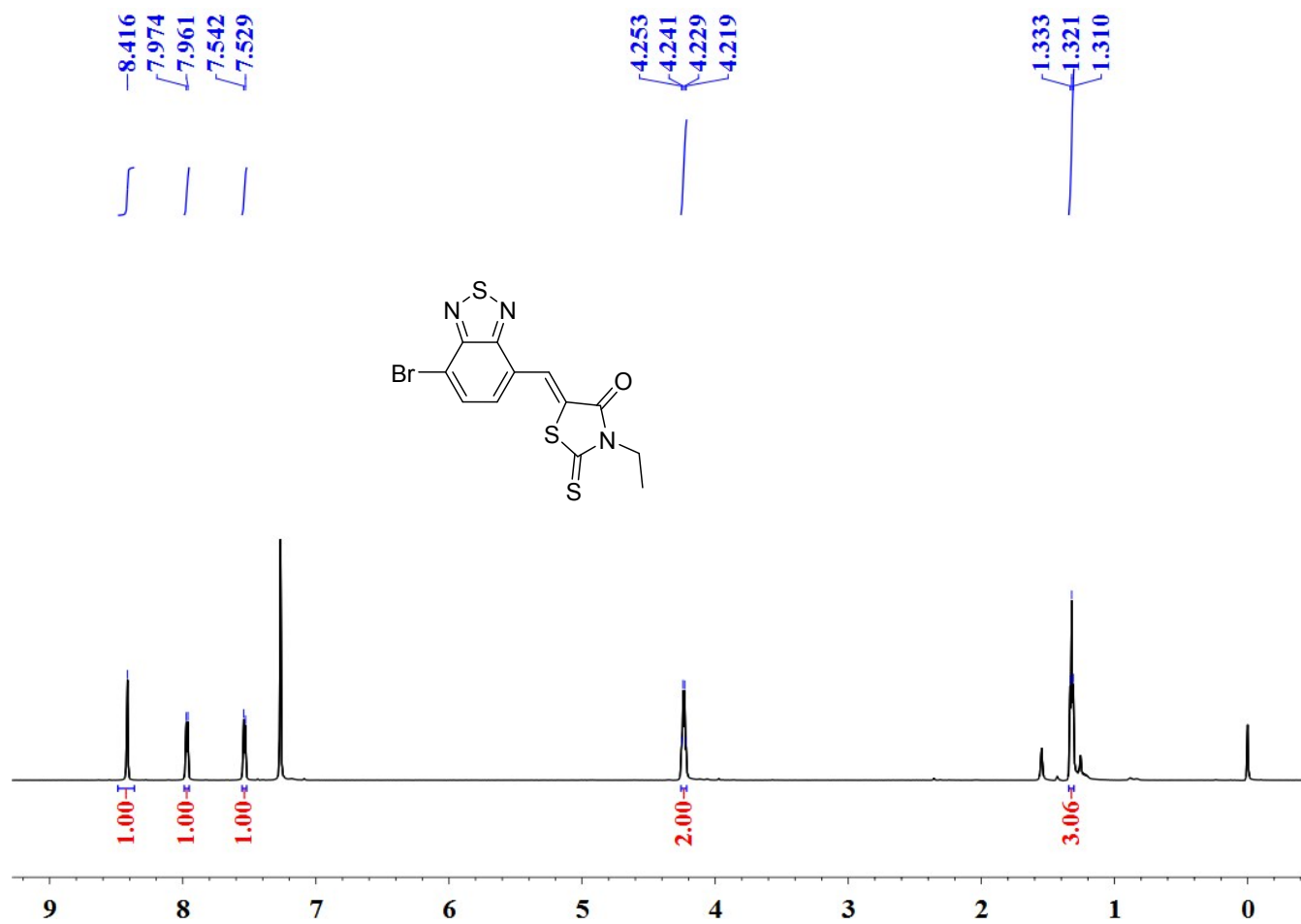
Figure S13. ^{1}H NMR spectrum of **2** in CDCl$_3$.
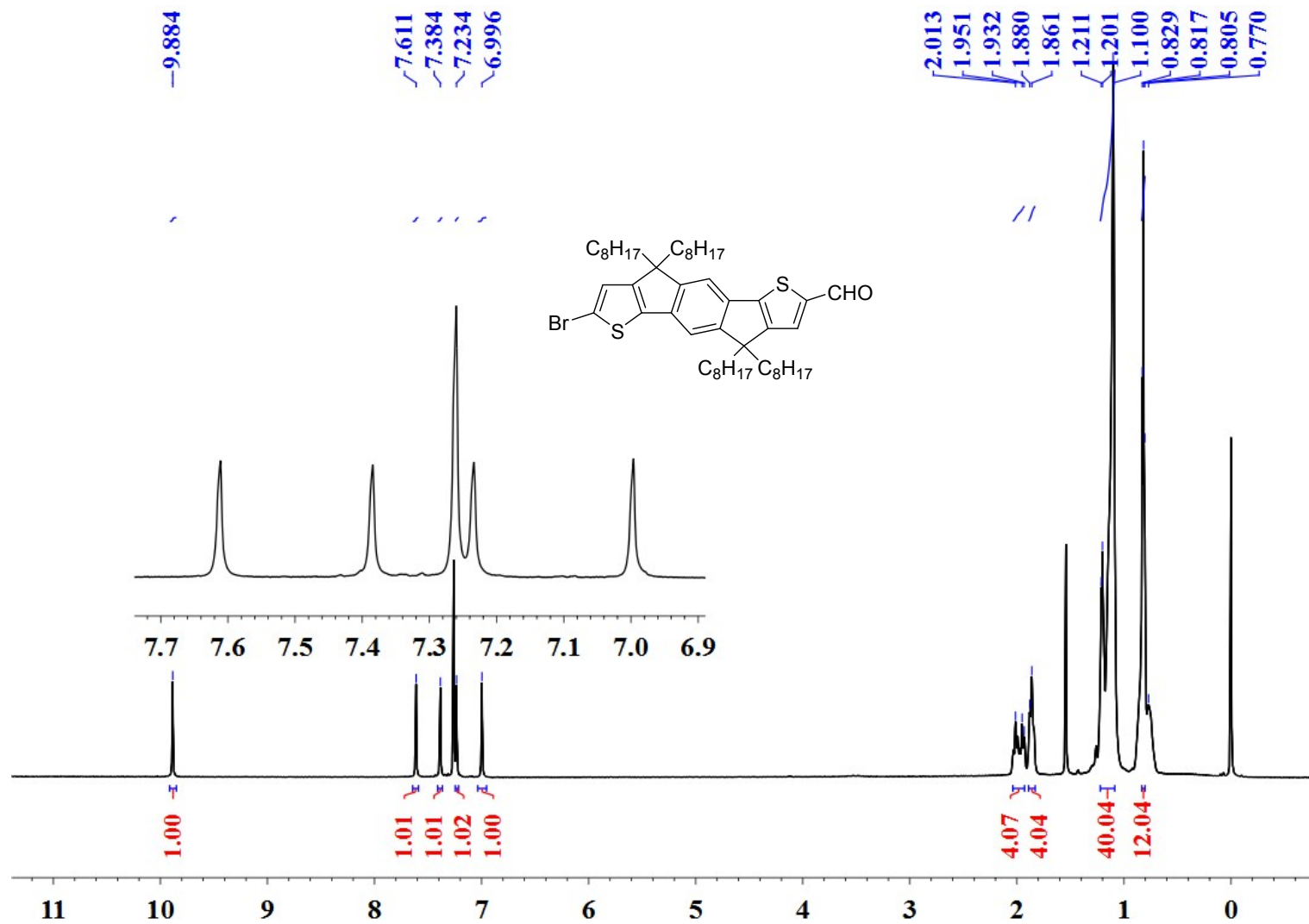
Figure S14. ^{1}H NMR spectrum of **4** in CDCl$_3$.
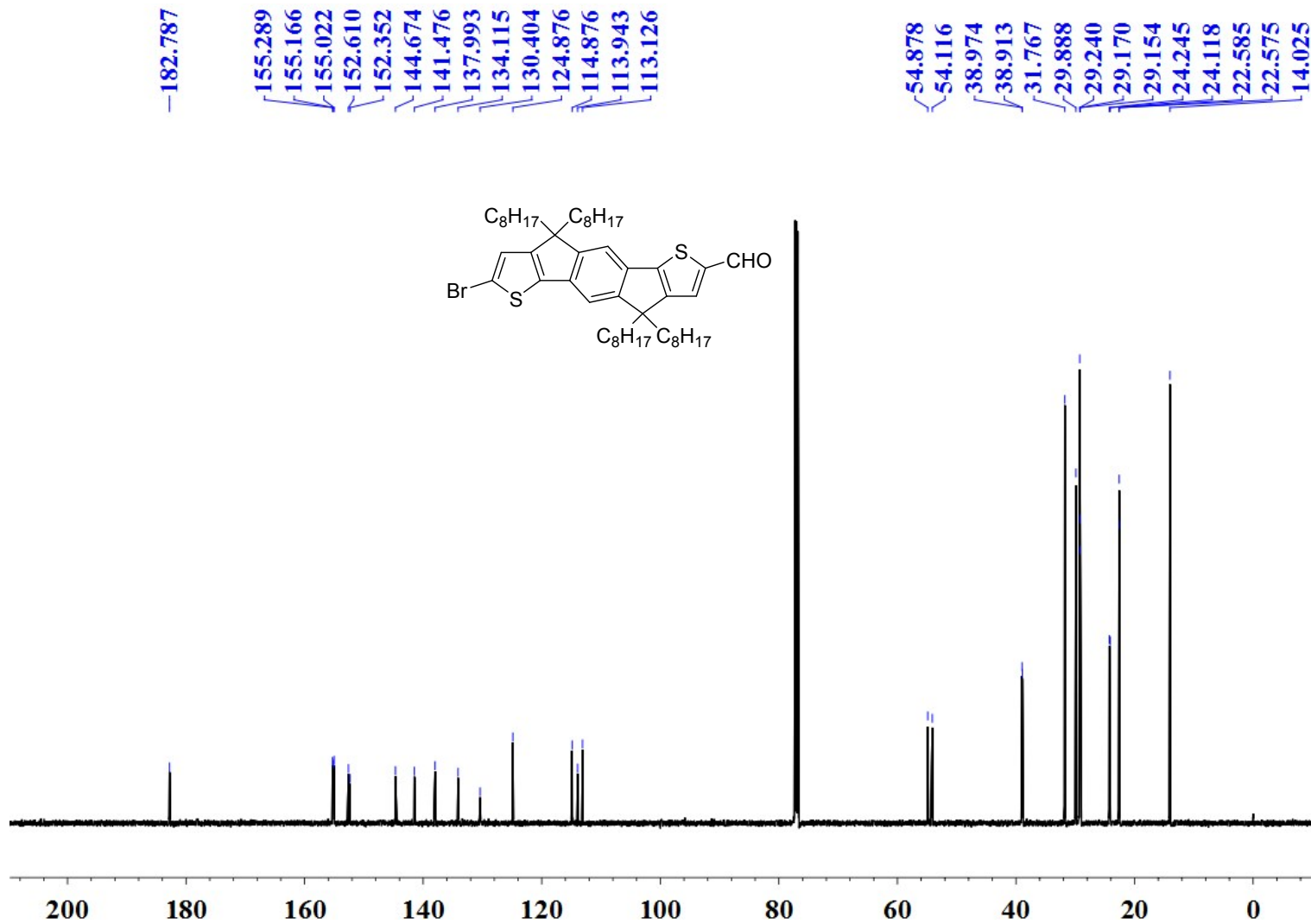
Figure S15. ^{13}C NMR spectrum of **4** in CDCl$_3$.
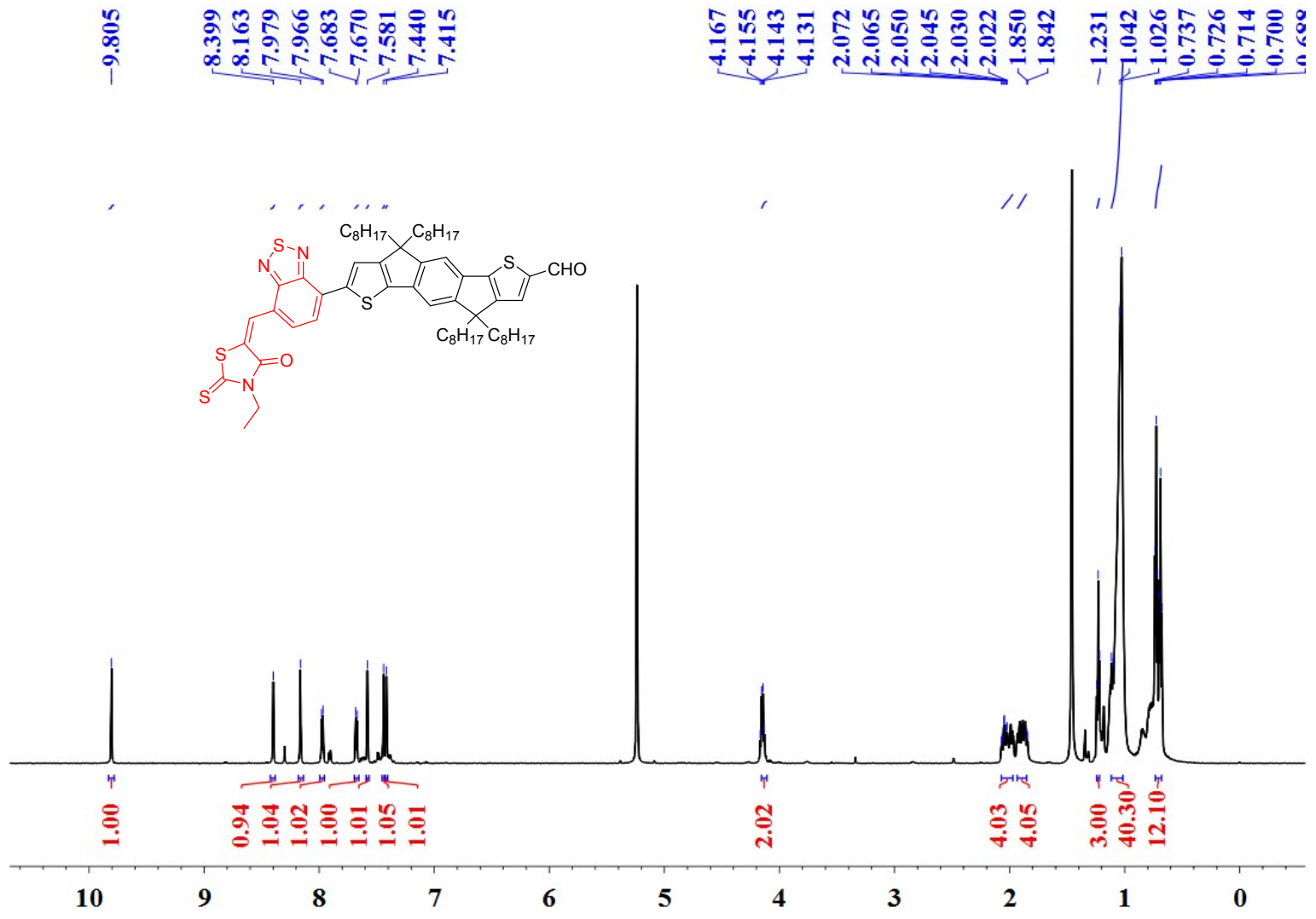
Figure S16. ^{1}H NMR spectrum of **5** in CD$_2$Cl$_2$.
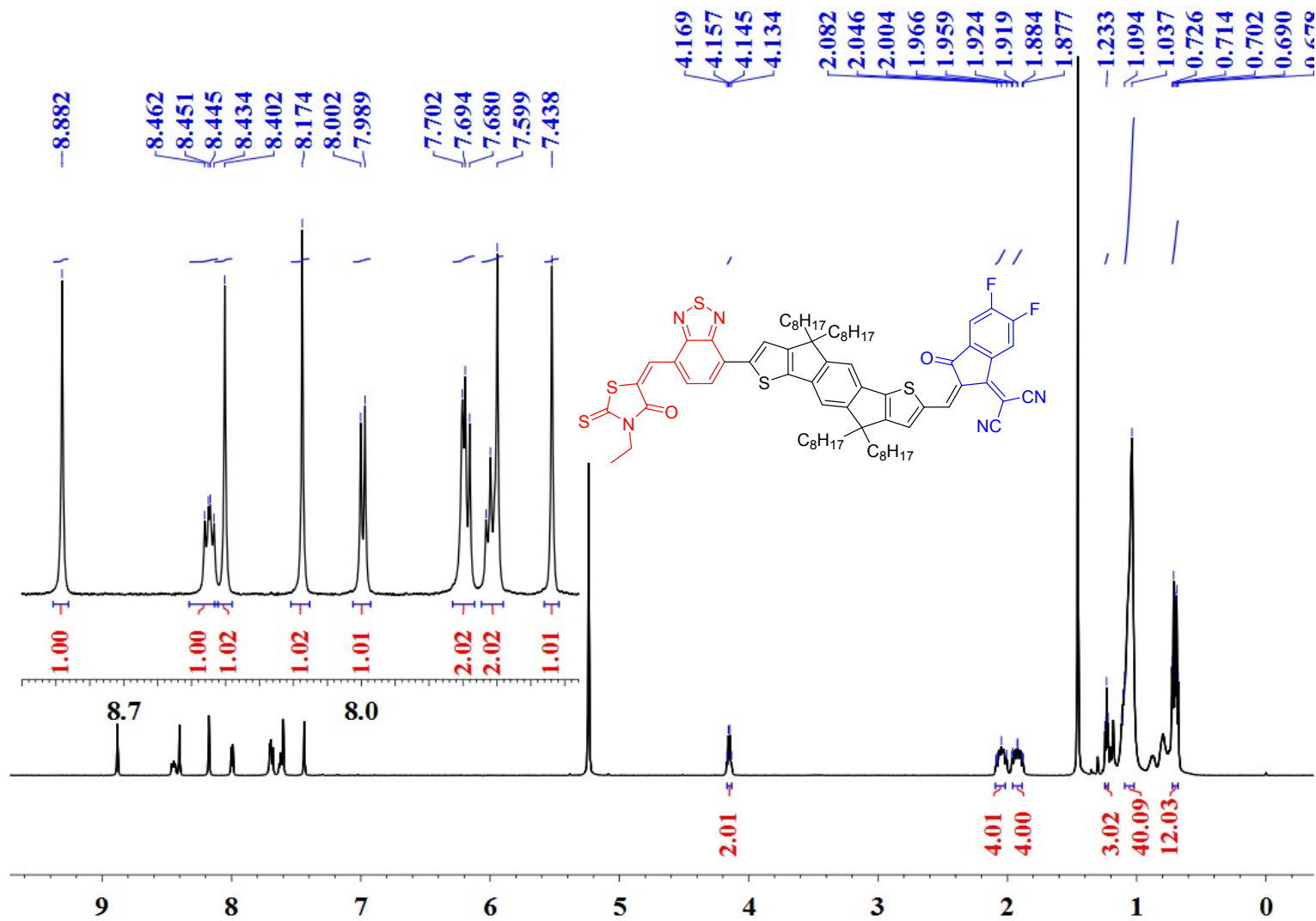
Figure S17. ^{1}H NMR spectrum of **IDTBF** in CD$_2$Cl$_2$.
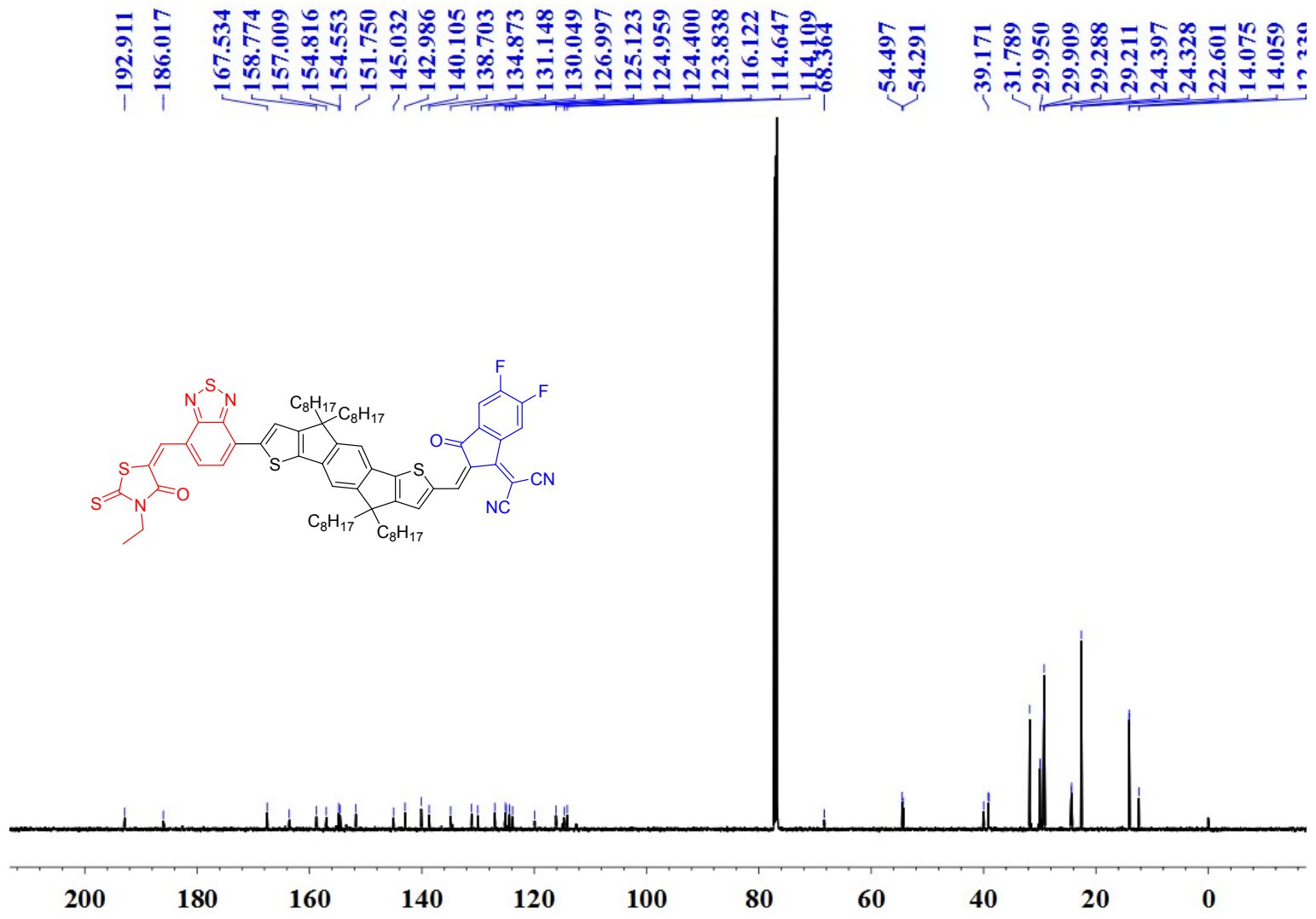
Figure S18. ^{13}C NMR spectrum of **IDTBF** in CDCl$_3$.
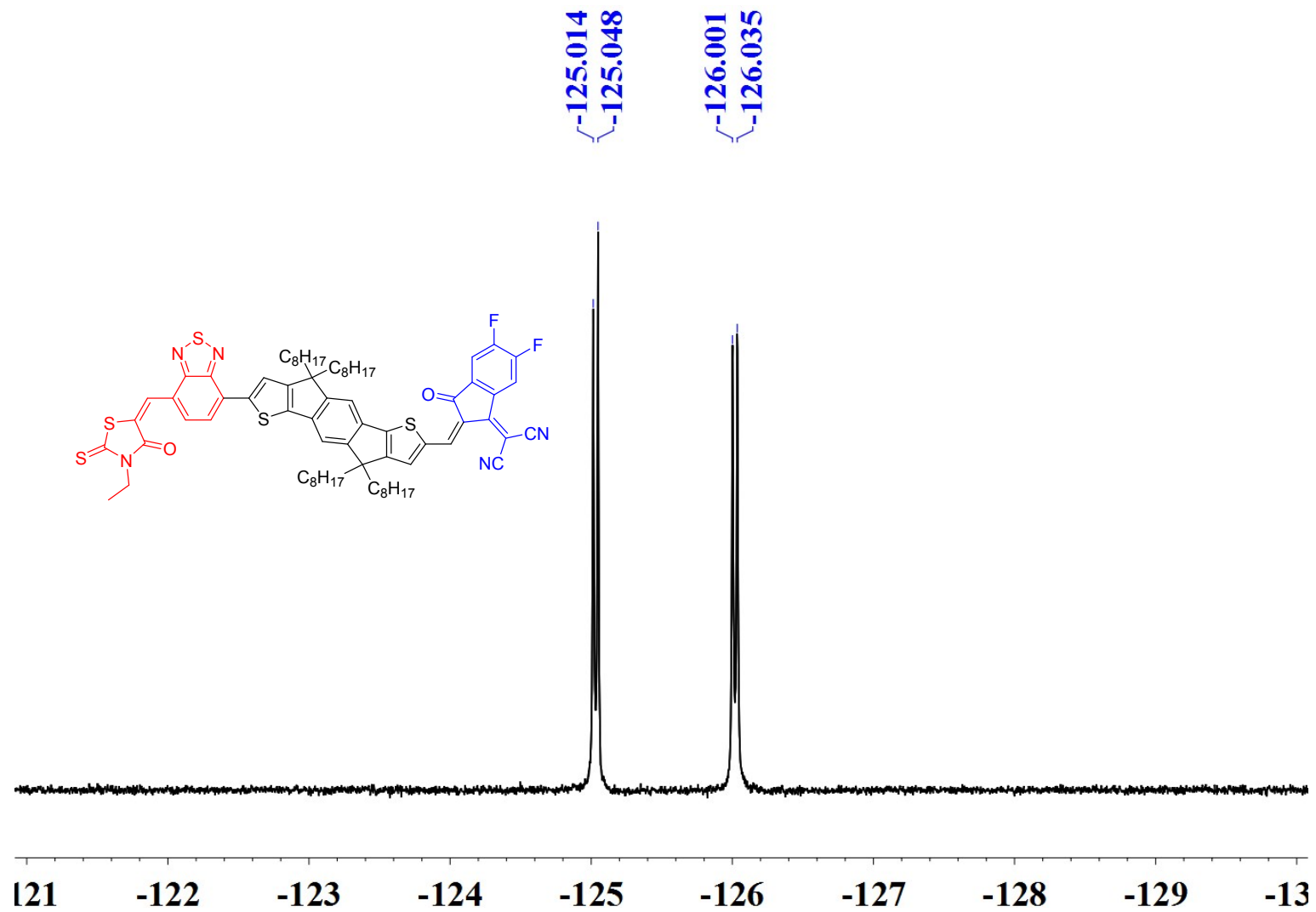
Figure S19. ^{19}F (^{1}H decoupled) NMR spectrum of **IDTBF** in CD_2Cl_2.

ESI Multistage MS/MS (SORI CID)

Analysis Info

				Acquisition Date	4/21/2020 2:13:45 PM
Analysis Name	D:\Data\S-TEST20200421\CC-4_000001.d				
Method	4_17_mass_range_pos_7T			Operator	
Sample Name	NaTFA			Instrument	solariX
Comment	0.1mg/ml NaTFA, 11.Dec.2013				

Acquisition Parameter

Polarity	Positive	n/a	n/a	No. of Laser Shots	200	
n/a	n/a	No. of Cell Fills	1	Laser Power	33.0 lp	
Broadband Low Mass	92.0 m/z	n/a	n/a	n/a	n/a	
Broadband High Mass	1000.0 m/z	n/a	n/a	n/a	n/a	
Acquisition Mode	Single MS	n/a	n/a			
Pulse Program	basic	n/a	n/a	Calibration Date	Tue Apr 21 12:01:38 2020	
Source Accumulation	0.000 sec	n/a	n/a	Data Acquisition Size	4194304	
Ion Accumulation Time	0.300 sec	n/a	n/a	Apodization	Sine-Bell Multiplication	
Flight Time to Acq. Cell	0.001 sec					
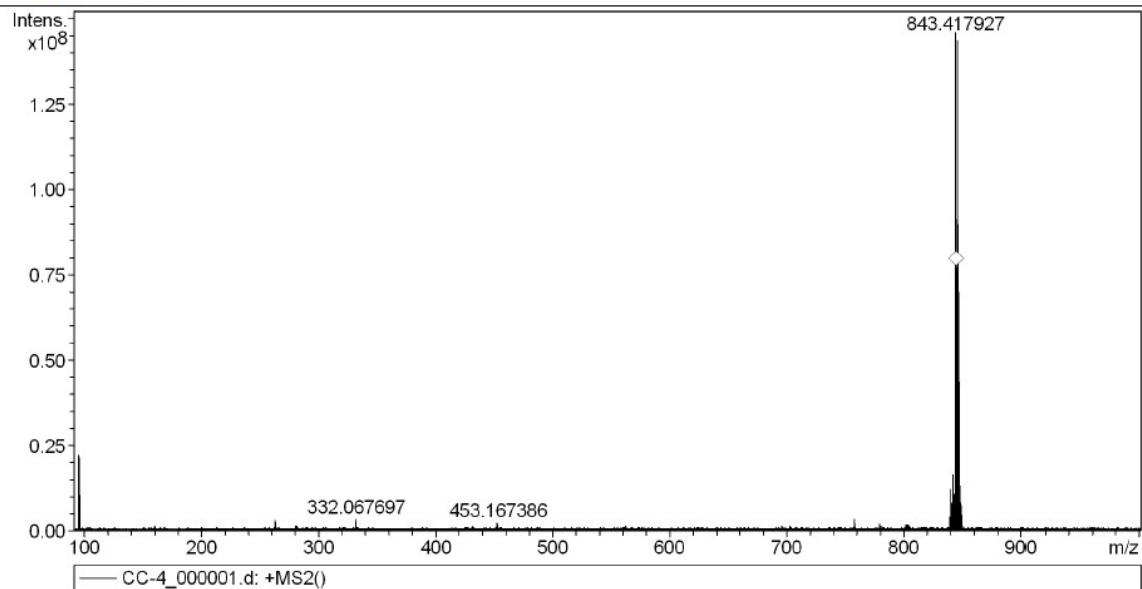
Figure S20. HR-MS spectrum of compound **4** ([M+Na]$^+$).

Mass Spectrum List Report

Analysis Info

				Acquisition Date	1/11/2020 3:25:33 PM
Analysis Name	D:\Data\HYY\BS_0_F11_000014.d				
Method	TY-8.31			Operator	
Sample Name				Instrument	solariX
Comment	PeptideMix NS=8 TF=1.2				

Acquisition Parameter

Polarity	Positive	n/a	n/a	No. of Laser Shots	100
n/a	n/a	No. of Cell Fills	1	Laser Power	70.0 lp
Broadband Low Mass	53.8 m/z	n/a	n/a	n/a	n/a
Broadband High Mass	2500.0 m/z	n/a	n/a	n/a	n/a
Acquisition Mode	Single MS	n/a	n/a		
Pulse Program	basic	n/a	n/a	Calibration Date	Fri Feb 21 02:36:54 2014
Source Accumulation	0.100 sec	n/a	n/a	Data Acquisition Size	1048576
Ion Accumulation Time	0.500 sec	n/a	n/a	Apodization	Sine-Bell Multiplication
Flight Time to Acq. Cell	0.001 sec	n/a	n/a	Apodization	Apodization
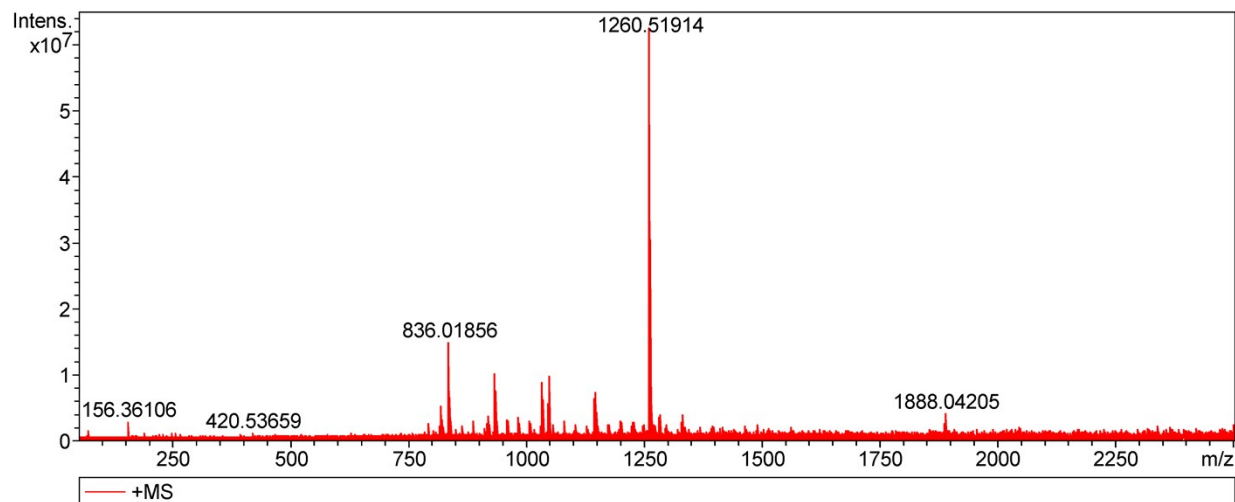
Figure S21. HR-MS spectrum of **IDTBF** ([M+H]$^+$).

15. FT-IR Spectra
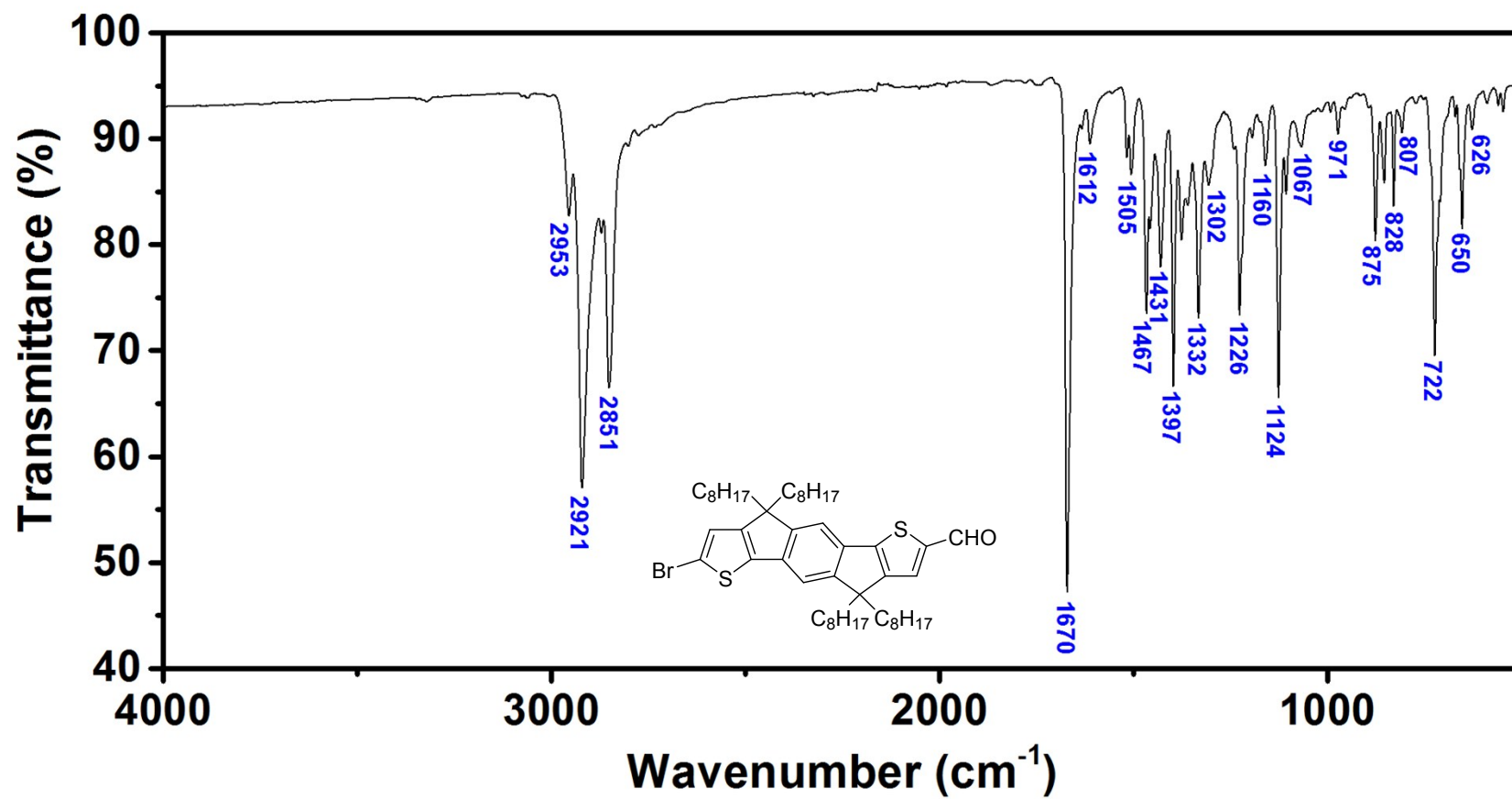
Figure S22. FT-IR spectrum of compound **4**.
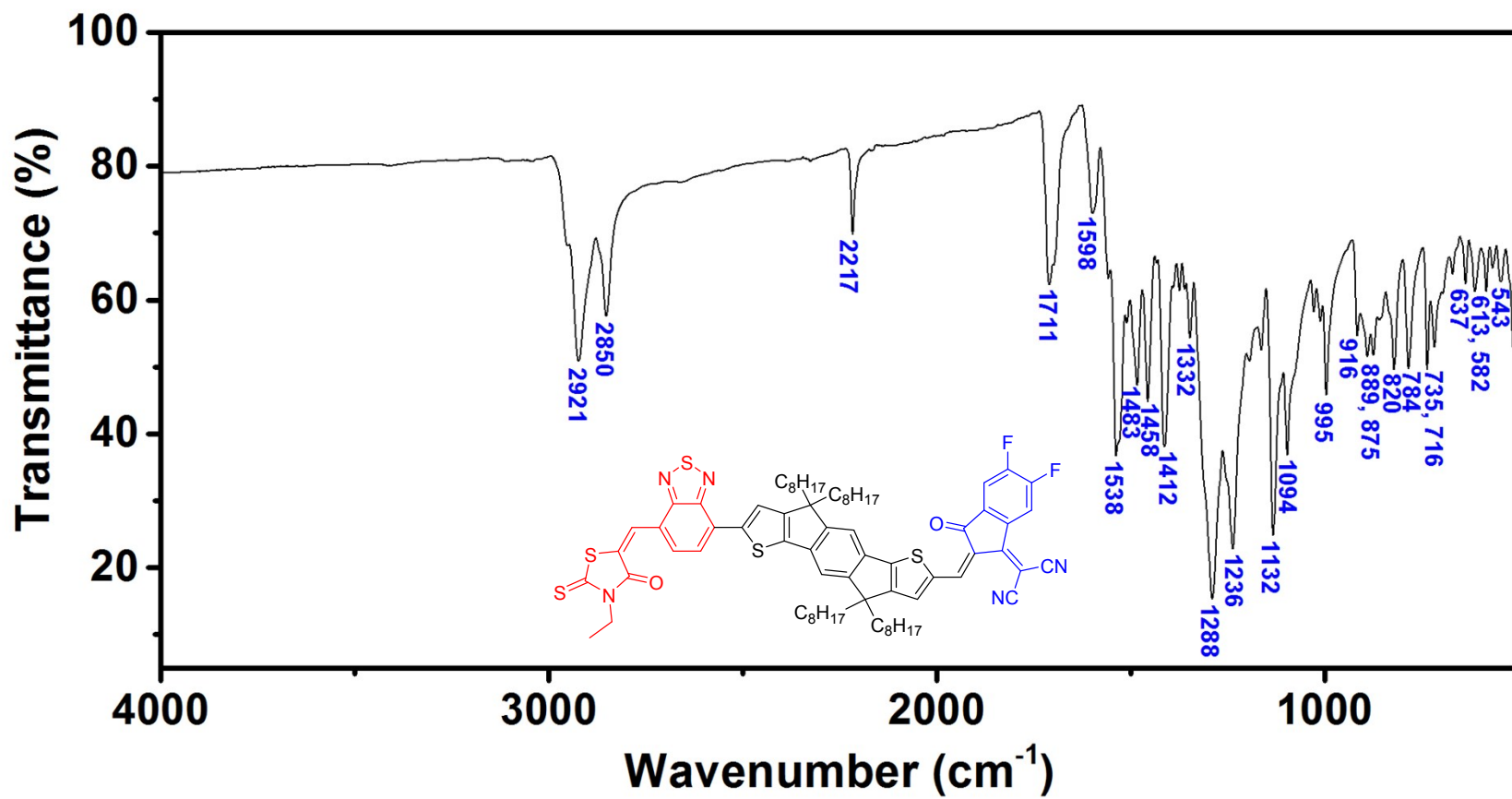
Figure S23. FT-IR spectrum of **IDTBF**.

16. References

[1] W. Mitchell, L. C. Chen, T. Cull, *PCT Int. Appl.* **2018**, WO2018065352A1.

[2] J. Pommerehne, H. Vestweber, W. Guss, R. F. Mahrt, H. Bassler, M. Porsch, J. Daub, *Adv. Mater.* **1995**, *7*, 551-554.